

# FINAL DESIGN OF CARIE PHOTOINJECTOR CAVITY WITH PLUG INSERT \*

H. Xu<sup>†</sup>, A. Alexander, P. M. Anisimov, G. Bustos, W. Choi, T. Grumstrup, S. Rocha, E. I. Simakov,  
T. Tajima, Los Alamos National Laboratory, Los Alamos, USA  
G. Lawler, J. Rosenzweig, University of California, Los Angeles, Los Angeles, USA

## Abstract

At Los Alamos National Laboratory (LANL), we finalized the design of a 1.6-cell C-band RF photoinjector cavity for the Cathodes And Radiofrequency Interactions in Extremes (CARIE) project. The photoinjector cavity is intended to operate at 5.712 GHz, with an intense electric field on the photocathode up to 240 MV/m, producing 250-pC electron bunches at room temperature. The photoinjector cavity design focused on minimizing the peak electric and magnetic fields. The distributed RF coupling waveguide network design was optimized for achieving minimized vacuum pressure at the photocathode plug emitting surface. Mechanical design considerations included photocathode plug alignment and symmetric ports for incident and reflected laser. The photoinjector was fabricated and was received at LANL in July 2025. In this paper, we report the design, fabrication, and preliminary low-power test results for the photoinjector.

## INTRODUCTION

At Los Alamos National Laboratory (LANL), a C-band (5.712 GHz) radiofrequency (RF) photoinjector cavity was developed for testing advanced photocathodes under high accelerating gradients at room temperature. The testing will be performed at the Cathodes And Radiofrequency Interactions in Extremes (CARIE) test stand [1, 2]. We expect to achieve electric field magnitude of 100–240 MV/m at the center of the cathode. The RF photoinjector cavity was fabricated by Dymenso, LLC, located in San Francisco, USA, and received at LANL in July 2025. The cavity is currently under low-power characterization and tuning. A photograph of the photoinjector cavity is shown in Fig. 1.

The 5.712-GHz standing-wave RF photoinjector cavity uses a 1.6-cell,  $\pi$ -mode geometry, which was originally proposed at University of California, Los Angeles (UCLA) [3]. The cell profile optimization for peak electric field mitigation and shunt impedance maximization was provided by SLAC National Accelerator Laboratory. The distributed RF coupling design, photocathode plug insertion geometry in the cavity, and the mechanical engineering and design were completed at LANL. The photocathode plug design was originally invented at INFN, later modified at SLAC. We further revised the plug tip geometry for the CARIE test stand at LANL.

\* Work supported by U.S. Department of Energy through the Laboratory Directed Research and Development program of Los Alamos National Laboratory, under project number 20230011DR.

<sup>†</sup> haoranxu@lanl.gov

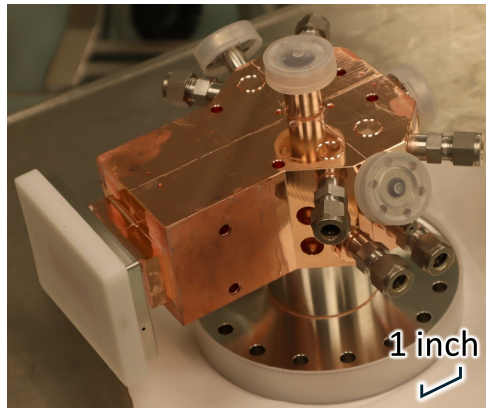


Figure 1: Photograph of the CARIE C-band (5.712 GHz) photoinjector cavity received at LANL.

## CAVITY DESIGN

The C-band photoinjector cavity design is illustrated in the three-quarter cross section view in Fig. 2. The cavity was modeled in SolidWorks. The cavity was designed to be fabricated as a brazed assembly of four copper quadrants. The four-quadrant brazing method was applied to fabricate all the features of this new design. In each cell of the cavity, three symmetry stubs were designed to eliminate the dipole mode content of the RF fields; electron beam numerical simulations showed that this geometry significantly reduced the output electron beam emittance [4, 5]. Meanwhile, compared to the previous design [4], the RF coupling waveguide network has been modified to maximize the vacuum conductance for the cathode cell. The vacuum flange on the

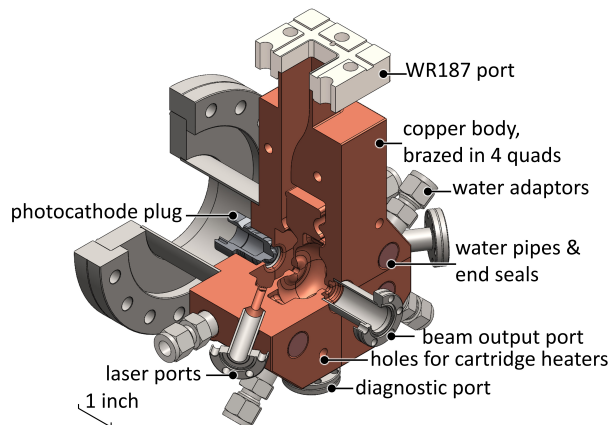


Figure 2: Three-quarter cross section view of the CARIE C-band standing-wave photoinjector design in SolidWorks.

back has an outer diameter of 6 inch (DN100CF), which will be connected to the photocathode load lock system. The rectangular WR187 waveguide port feeds microwave power to the cavity. The laser input and output are through the mini ConFlat flange ports on the side, and the 304 stainless steel laser pipes are brazed onto the copper body.

Iterative radiofrequency design and mechanical design were performed to ensure that a self-consistent and appropriate mechanical 3D model was produced for allowing feasible machining as well as four-quadrant brazing.

The finalized photocathode insertion geometry is provided in Fig. 3. The knife edge is made of 304 stainless steel. It defines the longitudinal position of the photocathode plug and provides RF seal between the photocathode plug and the photoinjector cavity. The knife edge allows the plug to be pushed with a force up to 50 N before reaching the yield strength. There was a trade-off between the plug tip fillet size and the emitting face electric field uniformity. The gap between the plug tip and the copper wall was enlarged for the purpose of suppressing electron multipactor. On the back side of the plug insertion geometry, a tapered guide is used to gradually center the photocathode plug during insertion, ensuring the alignment when the plug meets the knife edge. At the assembled position, in the transverse directions, the plug position (alignment) is defined by the single-point contacts with each copper quadrant; this design meanwhile ensures the vacuum conductance for the volume between the plug and the back side of the knife edge.

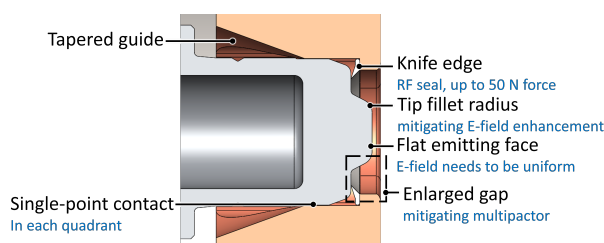


Figure 3: Half section view of the photocathode plug insertion geometry of the CARIE photoinjector.

The CST High Frequency Solver simulation results of the RF field distributions in the photoinjector cavity are shown in Fig. 4. In these plots, the electric field magnitude at the center of the cathode is 240 MV/m. The cavity operates at critical coupling. The waveguide network system ensures that the RF phase delay between the two cells is 180 degrees, and the arc-shaped choke at the top of the split waveguide leading to the cathode cell controls the proper power distribution so that the peak surface electric fields in the two cells are equal. In Fig. 4, the surface peak electric field is 316.8 MV/m, located at the re-entrant profiles of the two cells; the surface peak magnetic field is 478.0 kA/m, located at the coupling port from the split waveguide into the cathode cell, which results in a pulsed temperature rise of 48 K.

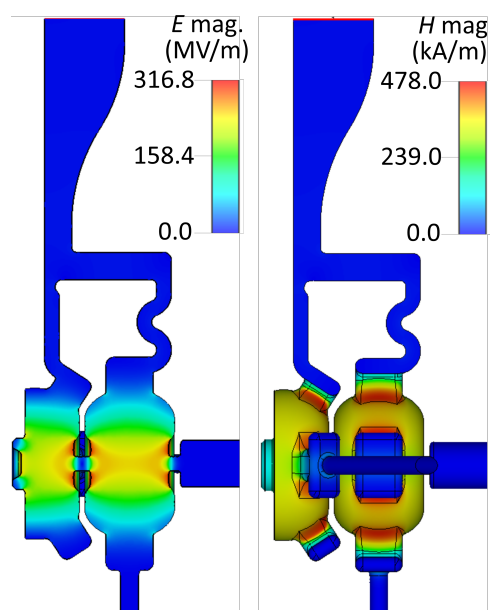


Figure 4: CST High Frequency Solver results of the electric (left) and magnetic (right) field distributions of the CARIE C-band photoinjector cavity, when the photocathode center witnesses an electric field magnitude of 240 MV/m.

## PRELIMINARY LOW-POWER TEST

The low-power characterization of the CARIE C-band photoinjector cavity as received was performed. Before the test, we installed a copper photocathode plug into the photoinjector cavity. This test plug was specially fabricated for the low-power test, with a tiny (0.7-mm diameter) hole drilled at the center for the nylon thread used in the field measurement (“bead pull”). For the high-power test, we will install another photocathode plug machined without this aperture at the center. In the preliminary low-power test of the photoinjector cavity, the scattering parameter and the electric field profile were measured.

The reflection coefficient  $S_{11}$  was measured, and the data is shown in Fig. 5, compared to the CST simulation result. During the low-power test, the cavity was first oriented in the horizontal direction for the initial  $S_{11}$  measurement, and then oriented in the vertical direction for the on-axis electric field measurement. Therefore, two sets of  $S_{11}$  measurements were performed. On the smith chart, it can be discerned that the resonant frequencies of the two cells were different by a very small amount; however, on the magnitude plot, due to that the resonant frequencies of the two cells were very close, only one resonant frequency can be identified, which agreed very well with the CST simulation result. It is remarkable that the cavity fabricated with such complex machining and brazing, as received and assembled with the photocathode plug for the first time, demonstrated resonant frequencies of the individual cells and RF coupling in excellent agreement with the theoretical predictions.

The field measurement (“bead pull”) of the photoinjector cavity was then performed, and the result is shown in Fig. 6,

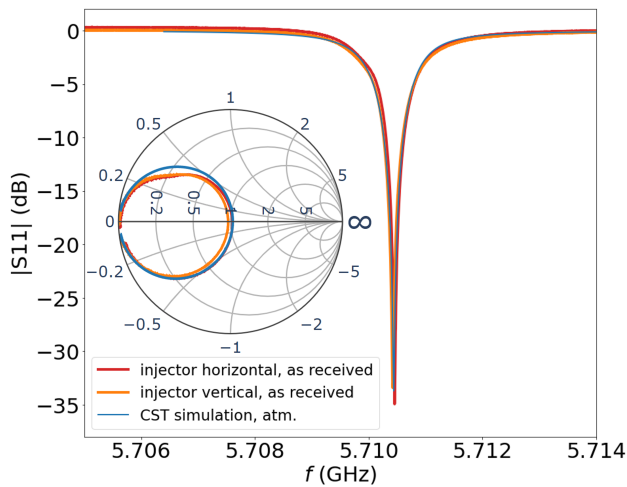


Figure 5: Reflection coefficient ( $S_{11}$ ) as measured in the newly received CARIE C-band photoinjector cavity, in comparison to the CST simulation result.

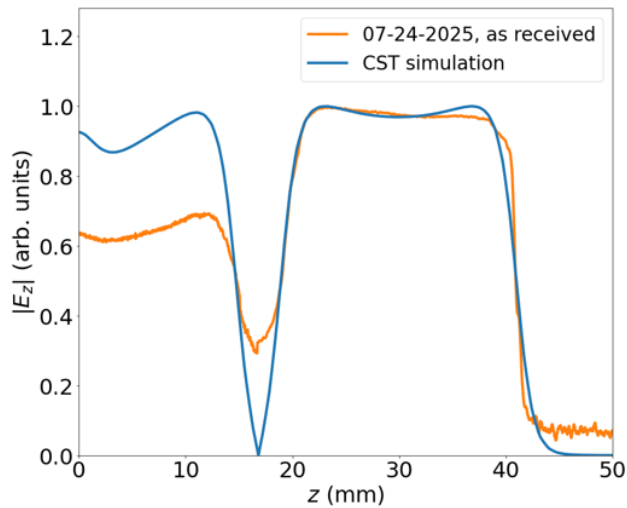


Figure 6: Electric field magnitude measurement result of the newly received CARIE C-band photoinjector cavity, in comparison to the CST simulation result.

compared to the CST simulation result. The processed result showed that the field magnitude in the cathode cell was lower than the CST prediction by 32%. Therefore, fine tuning must be performed to ensure that the RF fields in the two cells are balanced. Meanwhile, the measured RF phase of the full cell was 183.0 degrees behind that of the cathode cell, which was very close to the design value of 180.0 degrees.

Lastly, a summary of the as-received CARIE C-band photoinjector cavity low power test results is provided in Table 1. The results showed generally good agreement with the CST simulation results.

## CONCLUSIONS

A 1.6-cell C-band high-gradient radiofrequency photoinjector cavity was designed at Los Alamos National Laboratory for testing advanced photocathodes at high accelerating Table 1: CARIE C-band photoinjector cavity low-power experimental (as received, horizontal orientation) results and comparison to theory (in air).

Parameter	Exp.	Theory	Unit
resonant frequency	5710.46	5710.40	MHz
unloaded $Q_0$	10292	11510	
coupling fac. $\beta$	1.03	1.01	
norm. cath. E-field	0.63	0.93	arb. units
phase advance	183.0	180.0	deg

gradients. The photoinjector cavity has been fabricated, and the low-power characterization is underway.

The design of the photoinjector cavity was performed as a series of iterations of radiofrequency design adjustments and 3D mechanical modeling, with the goal of achieving the desirable beam dynamics and ensuring that the design was feasible for fabrication.

Low-power test results of the as-received photoinjector cavity were in very good agreement with the theoretical predictions. Fine tuning will be performed to balance the electric field magnitude in the two cells.

## REFERENCES

- [1] W. Choi *et al.*, “Progress on commissioning of the CARIE facility at LANL,” presented at 2025 North American Particle Accelerator Conference. (NAPAC’25), Sacramento, USA, Aug. 2025, paper WEP072, this conference.
- [2] E. Simakov *et al.*, “Status of the CARIE high gradient photocathode test facility at Los Alamos National Laboratory,” in *Proc. IPAC’25*, Taipei, Taiwan, Jun. 2025, pp. 883–886. doi:10.18429/JACoW-IPAC25-TUBD2
- [3] R. R. Robles *et al.*, “Versatile, high brightness, cryogenic photoinjector electron source,” *Phys. Rev. Accel. Beams*, vol. 24, no. 6, pp. 063401, 2021. doi:10.1103/PhysRevAccelBeams.24.063401
- [4] H. Xu *et al.*, “RF and multipactor analysis for the CARIE RF photoinjector with a photocathode insert,” in *Proc. IPAC’24*, Nashville, USA, May 2024, pp. 3251–3253. doi:10.18429/JACoW-IPAC2024-THPG04
- [5] P. M. Anisimov *et al.*, “Multi-objective genetic optimization of high charge TopGun photoinjector,” in *Proc. IPAC’24*, Nashville, USA, May 2024, pp. 840–843. doi:10.18429/JACoW-IPAC2024-MOPS55
- [6] CST Simulation Suite, <https://www.3ds.com/products/simulia/cst-studio-suite>